

## Treatment of a Biological Effluent Containing Metronidazole

Yerkanat N. Kanafin, Aliya Satayeva, Elizabeth Arkhangelsky, Stavros G. Pouloupoulos\*

School of Engineering and Digital Sciences, Environmental Science & Technology Group (ESTg), The Environment & Resource Efficiency Cluster (EREC), Nazarbayev University, Nur-Sultan, Kazakhstan  
stavros.pouloupoulos@nu.edu.kz

Emerging pollutants like metronidazole (MNZ) affect the removal efficiency of conventional activated sludge (CAS) based wastewater treatment plants and can escape traditional treatment facilities. Advanced oxidation processes (AOPs) and membrane filtration could complement the existing processes to completely eliminate pollutants of emerging concern in wastewaters. This work investigated the application of photochemical processes for treating a synthetic wastewater effluent from CAS treatment and membrane filtration of the biological effluents after CAS experiments with MNZ, caffeine (CAF) and ibuprofen (IBU). Photochemical experiments were conducted in a batch photochemical reactor. The influence of different chemical species such as  $H_2O_2$ , Fe(II),  $K_2S_2O_8$  and  $TiO_2$  and of pH value in the system were studied in terms of TOC removal and MNZ degradation. The application of UV/ $K_2S_2O_8$ /Fe(II) resulted in 78 % TOC removal in the effluent. Complete degradation of MNZ was observed after 30 min of treatment in the following experiments: UV/ $H_2O_2$ /Fe(II) at pH 3 and UV/ $K_2S_2O_8$ . Moreover, the effluents were treated by means of a membrane bioreactor (MBR). Polycarbonate track-etch membranes of 50 and 100 nm pore size were used. The results obtained showed that the carbon removal by the MBR was comparable with the conventional biological treatment. Rejection of MNZ depends on the presence/absence of other emerging contaminants in the wastewater effluents.

### 1. Introduction

MNZ is commonly used as an imidazole antibiotic, which is applied for treatment of the infections related to bacteria and protozoa in humans and animals. Its widespread usage and high solubility in water lead to the accumulation of metronidazole in aquatic environment. Metronidazole has been detected at different concentrations (1.8-9.4  $\mu\text{g/L}$ ) in hospital effluents and belongs to the class of the emerging pollutants (Alamgir et al., 2020). Due to the lymphocytic damage, metronidazole is a potentially human carcinogen and mutagen. Thus, it is essential to remove it from the industrial and municipal effluents before it enters the environment. However, the removal of metronidazole with conventional wastewater treatment techniques is complicated and inefficient due to its stable structure and high water solubility. For instance, only 34 % removal of metronidazole was measured at a large municipal wastewater treatment plant based on the activated sludge process in the Po Valley, northern Italy (Verlicchi et al., 2013). Wastewater treatment technologies such as AOPs and membrane filtration have been applied to treat MNZ-containing wastewater.

The term AOPs describes a large group of effective technologies used for the treatment of polluted drinking water and industrial wastewater. Generally, AOPs involve the generation of powerful oxidants like hydroxyl radicals and sulfate radicals. These oxidative radicals are capable of oxidizing various organic pollutants. The efficiency of AOPs depends on the radical generation rate and the extent of contact between the contaminant and the radical. Moreover, the presence of scavenging components such as carbonate or bicarbonate ions may affect the radical formation kinetics (Shemer et al., 2006). For example, Khataee et al. (2017) used photocatalytic ozonation with ZnO/Montmorillonite nanoparticles to achieve 97 % degradation of MNZ (40 mg/L) at pH 6 after 30 min of experiment. Application of photo-Fenton process (UV/ $H_2O_2$ / Fe(II)) by Shemer et al. (2006) resulted in 94 % degradation of MNZ (6  $\mu\text{M}$ ) at pH 3.5 after 5 min. Xia et al. (2019) treated MNZ

containing wastewater with electrochemical Fenton reaction at pH 3, and achieved 62.6 % removal of COD and 95 % degradation of MNZ (1000 mg/L) after 150 min.

Among commonly used treatment processes, membrane separation is presently recognized as the most efficient technology (Peter-Varbanets et al., 2009). MBR is a substitute for the activated sludge process, which has been the conventional wastewater treatment technique over the last one hundred years. Nowadays, MBR is an established and efficient technology that is used around the world. MBR is a hybrid system, which includes biological treatment and membrane filtration for physical liquid–solid separation. Conventional MBRs involve phase inversion membranes. However, phase inversion technique cannot produce pore size, geometry, density and pore size distribution in a controllable manner. Previously, it has been reported that track-etch technology is able to resolve this problem (Kozlovskiy, Zdorovets, & Arkhangelsky, 2017).

This work aimed at investigating the performance of AOPs and track-etch membrane separation processes for the treatment of wastewater containing MNZ. The efficiency of wastewater treatment technology was studied by measuring the concentration of MNZ and total organic carbon (TOC). To the best of authors' knowledge, there are no previous systematic and controlled studies on the performance of track etch membranes in MBRs and persulfate-based AOPs on the treatment of wastewater containing MNZ.

## 2. Materials and methods

### 2.1 Materials

Commercially available track-etch membranes (it4ip S.A., Belgium) were used in this study. The membranes were polycarbonate films with pore size of 50 or 100 nm. Hydrogen peroxide (37.6 % w/w) was received from Skat-Reaktiv. Hydrochloric acid (ACS reagent, 37 % w/w), titanium dioxide P-25 (nanopowder, ≥99.5 %, primary particle size: 21 nm), and potassium persulfate (≥99 %) were purchased from Sigma-Aldrich. All reagents were used as received without further purification.

### 2.2 Effluents' characteristics

Effluents were obtained after previous work with continuous flow activated sludge process (Kanafin et al., 2021). Synthetic wastewater effluent containing MNZ after CAS process followed by secondary clarifier was collected and used in the photochemical experiments. Effluents after CAS experiments with MNZ only and with three emerging pollutants such as MNZ, CAF and IBU were collected after the biological reactor and treated using membrane filtration. CAF and IBU weren't detected in the effluents after CAS treatment of MNZ, CAF and IBU. Characteristics of the effluents are shown in Table 1.

*Table 1: Effluents' characteristics*

Parameters	After CAS with MNZ	After CAS with MNZ, CAF and IBU	After CAS + clarifier
MNZ, mg/L	22.45	4.67	19.44
CAF, mg/L	0	0	0
IBU, mg/L	0	0	0
TC, mg/L	105.9	43.03	66.38 ± 0.79 %
TIC, mg/L	-	-	28.91 ± 0.37 %
TOC, mg/L	-	-	37.47
TN, mg/L	19.24	26.84	22.83 ± 0.59 %
pH	7.25	6.66	7.13

### 2.3 Analytical methods

Prior to the HPLC, TC, TIC and TN analysis, samples were filtered using Chromofil Xtra RC-20/25 syringe filters (0.20 µm), and diluted with ultra-pure water (Millipore Milli-Q Ultrapure Water Purification System, Germany). The determination of TC, TIC and TN was conducted using Multi N/C 3100 analyzer (Analytik Jena AG, Germany). Metronidazole was determined by the Agilent 1290 Infinity HPLC, USA. The pH was measured by WTW inoLab 9310 IDS, Germany. The samples for TSS and VSS determination were sampled twice and filtered through vacuum pump using 1.2 µm GF/F glass microfiber filters. TSS was measured by drying the sample in the oven until the constant weight. VSS was determined by calcination at 550 °C for 30 min. Infrared spectra of untreated and treated effluents were analyzed by FTIR spectrometer (Nicolet iS10, Thermo Fisher Scientific, USA) in the range of 4,000 - 400 cm<sup>-1</sup>.

## 2.4 Photochemical treatment experiments

The photochemical treatment was investigated with a batch photochemical reactor supplied by Toption (China). This essentially consisted of a 30 W lamp, which emitted UV light at the wavelength of 254 nm. The reactor was a cylindrical vessel of 400 mL effective volume. The first sample was taken when the UV light lamp was turned on. The solution in the reactor was continuously agitated by a magnetic stirrer. Samples for analysis were withdrawn from the reaction vessel every 30 min. Each experiment lasted 150 min. The electric energy per order,  $E_{EO}$  (kWh/m<sup>3</sup>/order), was estimated using Eq(1) for a batch reactor (Foteinis et al., 2018):

$$E_{EO} = \frac{P \cdot t \cdot 1000}{V \cdot 60 \cdot \log(C_i/C_f)} \quad (1)$$

where  $C_i$  and  $C_f$  are the initial and final concentration of pollutant (mg/L);  $P$  represents the electrical power of the UV lamp, kW;  $t$  stands for the irradiation time in min; and  $V$  is the volume of the treated wastewater, L.

## 2.5 Membrane filtration experiments

The biological reactor effluents were subjected to the membrane filtration. A peristaltic pump (Cole-Parmer Masterflex L/S, USA), membrane holder (Sterlitech, USA), electronic balance (OHAUS, USA), and stirrer plate were used in this study to construct the membrane filtration setup. The permeate collecting vessel was placed on the balance, while the feed was on the stirrer plate to provide a homogeneous solution. The experiments were implemented in dead-end mode through 4 x 4 cm<sup>2</sup> filtration area. The duration of each experiment was 6 hours. Membranes' zeta potential and contact angle were measured following the same protocol described earlier (Omir et al., 2020). The water flux was calculated gravimetrically.

## 3. Results and Discussions

### 3.1 Photochemical treatment of metronidazole containing CAS effluents

The infrared analyses of the untreated and treated effluents were conducted to explore the transformation of MNZ. As it can be seen from the infrared spectrum in Figure 1a, the peak located at 1,637 cm<sup>-1</sup> is due to the presence of aromatic ring in untreated effluents. In Figure 1b-c, the peaks observed at 1,637 cm<sup>-1</sup> and 1,636 cm<sup>-1</sup> indicate that the aromatic ring did not disappear during the photochemical treatment process and point to the incomplete mineralization of MNZ. The wide and strong absorption peaks observed in the range of 3,328 cm<sup>-1</sup> to 3,345 cm<sup>-1</sup> are due to the presence of -OH group (Xia et al., 2019).

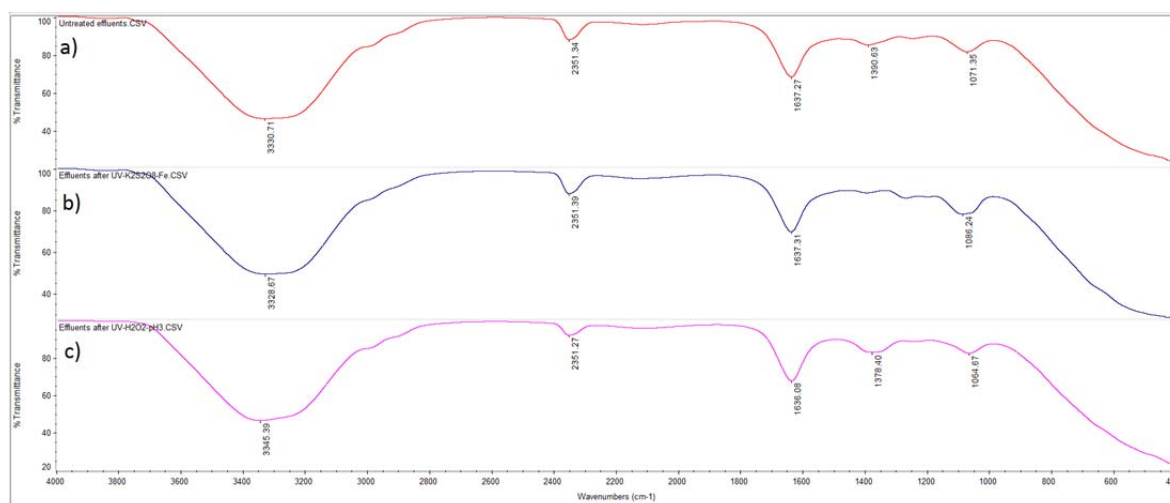


Figure 1: FT-IR analysis of (a) untreated effluents, (b) effluents after UV/K<sub>2</sub>S<sub>2</sub>O<sub>8</sub>/Fe(II) and (c) effluents after UV/H<sub>2</sub>O<sub>2</sub> at pH 3

Effluents were treated using  $\text{H}_2\text{O}_2$ ,  $\text{Fe(II)}$ ,  $\text{K}_2\text{S}_2\text{O}_8$  and  $\text{TiO}_2$  under UV irradiation. The TOC removal and MNZ degradation results are shown in Figure 2.

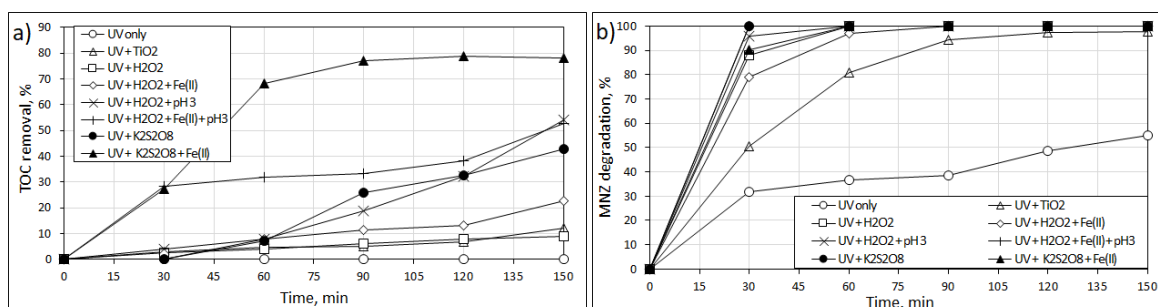


Figure 2: (a) TOC removal and (b) MNZ removal during photochemical treatment of MNZ containing effluents

As it can be seen from Figure 2a, the use of UV light alone did not lead to the complete mineralization of wastewater effluents. Similarly, the use of 8 mmol/L  $\text{H}_2\text{O}_2$  in UV/ $\text{H}_2\text{O}_2$  process was not capable of mineralizing the wastewater substantially (TOC removal 8 %). In contrast, the decrease of pH to 3 increased the efficiency of the UV/ $\text{H}_2\text{O}_2$  process, and resulted in 54 % TOC removal after 150 min. The adjustment of pH affects the composition and light absorption of the compounds in water. At acidic pH, pollutants present in water absorb a very small part of irradiation and thus the majority of irradiation contributes to the decomposition of hydrogen peroxide and production of hydroxyl radicals. Moreover, acidic pH leads to the reduction of TIC, which contains OH scavenging compounds (Philippopoulos and Pouloupoulos, 2003).

To improve the UV/ $\text{H}_2\text{O}_2$  process,  $\text{Fe(II)}$  5 mg/L was introduced in the next experiment, starting photo-Fenton reactions. The use of this process resulted in TOC removal of 23 %, while combining with the pH adjustment to 3 further increased the TOC removal up to 53 %. It should be noted that the photo-Fenton process is favoured at acidic pH values due to the increased solubility of iron. Moreover, the use of UV helps to avoid formation of iron organic complexes that may inhibit the regeneration of  $\text{Fe(II)}$  (Bello et al., 2019).

$\text{K}_2\text{S}_2\text{O}_8$  was used as another source of strong oxidizing radicals. Unlike OH radicals,  $\text{SO}_4^{2-}$  radicals are less affected by scavenging components (natural organic matter, alkalinity) in solution. The application of 5 mmol/L  $\text{K}_2\text{S}_2\text{O}_8$  under UV resulted in 43 % removal of TOC, while the use of photo-Fenton-like process (UV/ $\text{K}_2\text{S}_2\text{O}_8$ / $\text{Fe(II)}$ ) significantly contributed to the mineralization (TOC removal 78 %) of wastewater effluents. The generation of sulfate radicals decreased pH of the treated effluent solution down to 2.88, which was favourable for the regeneration of  $\text{Fe(II)}$  ions. Finally, photocatalytic experiments with 1 g/L of  $\text{TiO}_2$  yielded a 12 % TOC removal.

According to the results on MNZ degradation in Figure 2b, complete degradation of MNZ was achieved in the following experiments: UV/ $\text{H}_2\text{O}_2$ , UV/ $\text{H}_2\text{O}_2$ / $\text{Fe(II)}$ , UV/ $\text{H}_2\text{O}_2$  at pH 3, UV/ $\text{H}_2\text{O}_2$ / $\text{Fe(II)}$  at pH 3, UV/ $\text{K}_2\text{S}_2\text{O}_8$  and UV/ $\text{K}_2\text{S}_2\text{O}_8$ / $\text{Fe(II)}$ . UV light without any oxidant and UV/ $\text{TiO}_2$  processes degraded 55 % and 98 % of MNZ after 150 min of irradiation, respectively. The major fraction of operating costs of photochemical wastewater treatment relies on the energy consumption of ultraviolet lamp. The electric energy per order for a batch reactor was calculated from Eq(1). TOC values were used for  $C_i$  and  $C_f$ , and the results obtained are shown in Figure 3.

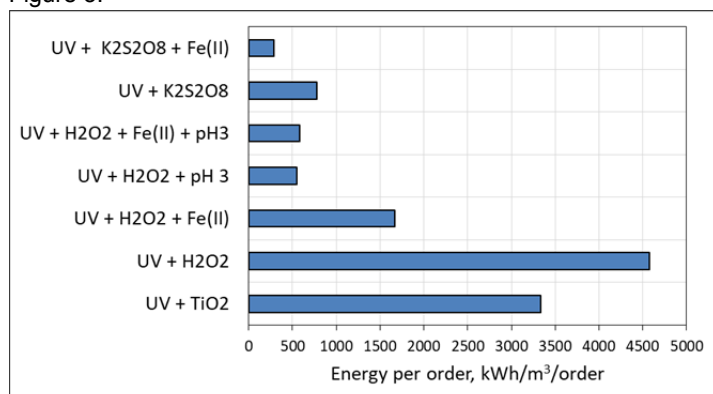


Figure 3: Energy per order for photochemical treatment of MNZ containing effluents

According to the calculations of the electric energy per order ( $E_{EO}$ , kWh/m<sup>3</sup>/order) using the TOC removal, the lowest  $E_{EO}$  value of 285 kWh/m<sup>3</sup>/order was observed for the UV/K<sub>2</sub>S<sub>2</sub>O<sub>8</sub>/Fe(II) process. The values obtained for persulfate oxidation were in the range of 285–774 kWh/m<sup>3</sup>/order. It can be seen that the addition of Fe(II) resulted in about 2.7 fold decrease of energy consumptions for both H<sub>2</sub>O<sub>2</sub> and K<sub>2</sub>S<sub>2</sub>O<sub>8</sub> driven systems. Similarly, the pH adjustment strongly contributed in the decrease of energy consumptions for UV/H<sub>2</sub>O<sub>2</sub> and UV/H<sub>2</sub>O<sub>2</sub>/Fe(II) processes.

### 3.2 Membrane treatment of metronidazole containing effluents

Table 2 demonstrates the results of membrane filtration after biological treatment.

Table 2: MNZ, TSS and VSS removal by the membranes.

Conditions	MNZ removal, %	TSS, g/L	VSS, g/L
before membrane, effluents after CAS with MNZ	-	2.46	2.1
before membrane, effluents after CAS with MNZ, CAF and IBU	-	1.74	1.69
after 50 nm membrane, effluents after CAS with MNZ	0	0.0003	0.0003
after 50 nm membrane, effluents after CAS with MNZ, CAF and IBU	100	0.0002	0.002
after 100 nm membrane, effluents after CAS with MNZ	0	0.0002	0.0003
after 100 nm membrane, effluents after CAS with MNZ, CAF and IBU	100	0.0017	0.0001

It can be seen that 50 and 100 nm membranes were not efficient in MNZ removal. On the other hand, when the effluent after CAS treatment of MNZ, CAF and IBU was used, the membranes showed 100 % retention of MNZ. TSS and VSS rejection consisted more than 99 % for both filters. In addition, the TC rejection by 100 nm MBR (effluents after CAS with MNZ) was found to be 69 %. This value is comparable with the TC removal of the CAS treatment of MNZ followed by secondary clarifier, which was 74 %. Similar results from the MBR and the conventional biological treatment for carbon retention can be explained by the relatively high pore size of membrane applied.

Figures 4 exhibits the water flux profiles and zeta potential for 50 nm and 100 nm membranes.

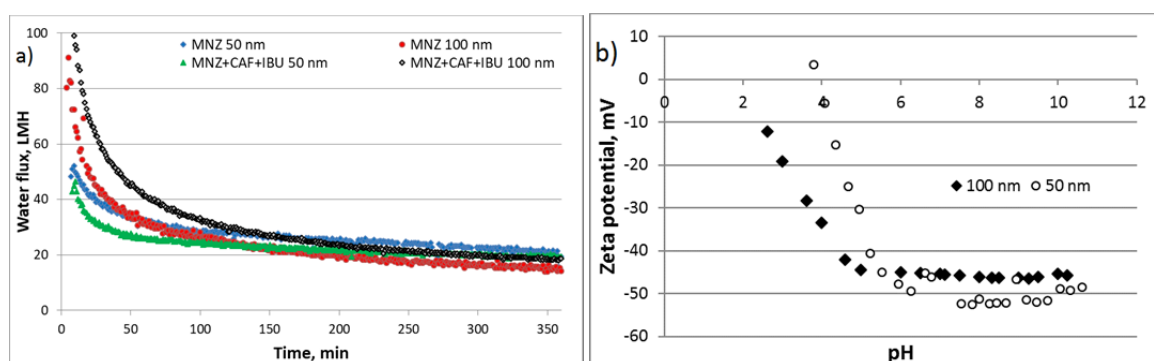


Figure 4: (a) Water flux during the membrane filtration (b) Zeta potential of the membrane with pore size of 50 nm and 100 nm at 1 mM KCl.

The initial water flux for 50 and 100 nm membranes was around 48 and 95 L/m<sup>2</sup>-h (LMH), respectively (Figure 4a). After 360 min of filtration, the water flux through all the membranes was 18 LMH on average. Comparing the initial and final flux values, it can be estimated that the water flux decline was 57 % for the 50 nm membrane and 83 % for the 100 nm membrane. Higher flux decline for the membrane with higher initial water flux is a result of increased foulants concentration on/within membrane, which is brought to the membrane by improved convective flow.

Membranes with 50 and 100 nm pore size were expected to demonstrate different performance. Indeed, the data obtained confirmed that the membranes used showed very different water flux profiles. However, MNZ, VSS and TSS removal results for both membranes were similar. Trying to explain this phenomenon membranes' zeta potential and contact angle were measured. The contact angles of the membranes with 50 nm and 100 nm pore sizes were 20° and 17°, respectively. This indicates hydrophilic nature of both membranes. The Figure 4b illustrates that with pH increase the zeta potential of both membranes becomes more electronegative. In the 6–10.5 pH range, the membranes had similar values of the zeta potential, i.e. around – 49 mV. In the 2.5–6 pH range, the filters demonstrated a quite different behaviour.

For instance, +3 – (–48) mV for 50 nm and (–12) – (–48) mV for 100 nm membrane. From the contact angle and zeta potential tests, it can be seen that the membranes possess similar charge and hydrophilicity. The similar charge for both membranes can be explained by the fact that the pH of the solution applied to the membranes was 7.1, while the zeta potential at pH 7.1 was equal to – 46 and – 52 mV. The experiments suggest the further investigation of MNZ removal mechanism in the presence of other contaminants of emerging concern and enhancing efficiency of the process by applying membranes with smaller pore size.

#### 4. Conclusions

In this study, AOPs and membrane filtration were used to treat biological effluents with MNZ. The main results are:

1. In the case of the photochemical treatment of the CAS effluents using UV/K<sub>2</sub>S<sub>2</sub>O<sub>8</sub>/Fe(II), the removal achieved was 100 % after 60 min for metronidazole and 78 % for TOC after 90 min.
2. The MBR demonstrated 69 % carbon removal and 100 % MNZ retention in the effluents after CAS experiments with MNZ, CAF and IBU.
3. The study showed that biological, AOP and membrane separation processes are efficient wastewater treatment technologies that require more attention thoroughly to understand removal mechanisms.

#### Acknowledgments

This work was supported by the Nazarbayev University project “Cost-Effective Photocatalysts for the Treatment of Wastewaters containing Emerging Pollutants”, Faculty development competitive research grants program for 2020-2022, Grant Number 240919FD3932.

#### References

- Alamgir, Talha K., Wang B., Liu J. H., Ullah R., Feng F., Yu J., Chen S., Li J. R., 2020, Effective adsorption of metronidazole antibiotic from water with a stable Zr(IV)-MOFs: Insights from DFT, kinetics and thermodynamics studies, *Journal of Environmental Chemical Engineering*, 8(1), 103642.
- Bello M.M., Abdul Raman A. A., Asghar A., 2019, A review on approaches for addressing the limitations of Fenton oxidation for recalcitrant wastewater treatment, *Process Safety and Environmental Protection*, 126, 119–140.
- Foteinis S., Borthwick A.G.L., Frontistis Z., Mantzavinos D., Chatzisyneon, E., 2018, Environmental sustainability of light-driven processes for wastewater treatment applications, *Journal of Cleaner Production*, 182, 8–15.
- Kanafin Y. N., Kakimov Y., Adamov A., Makhatova A., Yeshmuratov A., Pouloupoulos S.G., Inglezakis V.J., Arkhangelsky E., 2021, The effect of caffeine, metronidazole and ibuprofen on continuous flow activated sludge process, *Journal of Chemical Technology & Biotechnology*, 96(5), 1370-1380.
- Khataee A., Kıranşan M., Karaca S., Sheydaei M., 2017, Photocatalytic ozonation of metronidazole by synthesized zinc oxide nanoparticles immobilized on montmorillonite, *Journal of the Taiwan Institute of Chemical Engineers*, 74, 196–204.
- Kozlovskiy A., Zdorovets M., Arkhangelsky E., 2017, Track-etch membranes: The Kazakh experience, *Desalination and Water Treatment*, 76, 143–147.
- Omir A., Satayeva A., Chinakulova A., Kamal A., Kim J., Inglezakis V. J., Arkhangelsky, E., 2020, Behaviour of aquaporin forward osmosis flat sheet membranes during the concentration of calcium-containing liquids, *Membranes*, 10(5).
- Peter-Varbanets M., Zurbrügg C., Swartz C., Pronk W., 2009, Decentralized systems for potable water and the potential of membrane technology, *Water Research*, 43(2), 245–265.
- Philippopoulos C. J., Pouloupoulos S. G., 2003, Photo-assisted oxidation of an oily wastewater using hydrogen peroxide, *Journal of Hazardous Materials*, 98(1–3), 201–210.
- Shemer H., Kunukcu Y. K., Linden K. G., 2006, Degradation of the pharmaceutical Metronidazole via UV, Fenton and photo-Fenton processes, *Chemosphere*, 63(2), 269–276.
- Verlicchi P., Galletti A., Petrovic M., Barceló D., Al Aukidy, M., Zambello E., 2013, Removal of selected pharmaceuticals from domestic wastewater in an activated sludge system followed by a horizontal subsurface flow bed - Analysis of their respective contributions, *Science of the Total Environment*, 454–455, 411–425.
- Xia Y., Zhang Q., Li G., Tu X., Zhou Y., Hu X., 2019, Biodegradability enhancement of real antibiotic metronidazole wastewater by a modified electrochemical Fenton, *Journal of the Taiwan Institute of Chemical Engineers*, 96, 256–263.